Published in final edited form as:
Biochim Biophys Acta. 2010 ; 1797(6-7): 913–921. doi:10.1016/j.bbabio.2010.03.018.

Regulation of mitochondrial fission by intracellular Ca^{2+} in rat ventricular myocytes

Jennifer Hom[b], **Tianzheng Yu**[c,d], **Yisang Yoon**[a,c], **George Porter**[a,b], and **Shey-Shing Sheu**[a,¶]

[a]Department of Pharmacology and Physiology, Mitochondrial Research & Innovation Group, University of Rochester School of Medicine and Dentistry, Rochester, NY 14642, USA

[b]Department of Pediatrics, University of Rochester School of Medicine and Dentistry, Rochester, NY 14642, USA

[c]Department of Anesthesiology, University of Rochester School of Medicine and Dentistry, Rochester, NY 14642, USA

Abstract

Mitochondria are dynamic organelles that constantly undergo fission, fusion, and movement. Increasing evidence indicates that these dynamic changes are intricately related to mitochondrial function, suggesting that mitochondrial form and function are linked. Calcium (Ca^{2+}) is one signal that has been shown to both regulate mitochondrial fission in various cells types and stimulate mitochondrial enzymes involved in ATP generation. However, although Ca^{2+} plays an important role in the adult cardiac muscle cells for excitation-metabolism coupling, little is known about whether Ca^{2+} can regulate their mitochondrial morphology. Therefore, we tested the role of Ca^{2+} in regulating cardiac mitochondrial fission. We found that neonatal and adult cardiomyocyte mitochondria undergo rapid and transient fragmentation upon a thapsigargin (TG)- or KCl-induced cytosolic Ca^{2+} increase. The mitochondrial fission protein, DLP1, participates in this mitochondrial fragmentation, suggesting that cardiac mitochondrial fission machinery may be regulated by intracellular Ca^{2+} signaling. Moreover, the TG-induced fragmentation was also associated with an increase in reactive oxygen species (ROS) formation, suggesting that activation of mitochondrial fission machinery is an early event for Ca^{2+}-mediated ROS generation in cardiac myocytes. These results suggest that Ca^{2+}, an important regulator of muscle contraction and energy generation, also dynamically regulates mitochondrial morphology and ROS generation in cardiac myocytes.

Keywords

Mitochondria; mitochondrial fusion and fission; calcium; ventricular myocytes; reactive oxygen species; cardiac muscle

[¶]To whom correspondence should be sent: Shey-Shing Sheu, Ph.D., 601 Elmwood Ave, Box 711, Rochester, NY 14642, TEL: (585) 275-3381, FAX: (585) 273-2652, sheyshing_sheu@urmc.rochester.edu.
[d]Current address: Alfaisal University College of Medicine, Riyadh 11533, Kingdom of Saudi Arabia tyu@alfaisal.edu

1. INTRODUCTION

Cardiac myocytes, with their high metabolic demands, are comprised of approximately 35% mitochondrial volume per cell [1]. These mitochondria, mostly situated among the contractile filaments and next to the sarcoplasmic reticulum (SR), perform the important role of providing ATP and regulating Ca^{2+} in microdomains [2]. Mitochondrial shape varies greatly within the adult cardiomyocyte. Based on electron microscopic observations, interfibrillar mitochondria are relatively large and oval shaped and evenly distributed in a crystal-like pattern along the contractile apparatus, whereas the subsarcolemmal and perinuclear mitochondria vary in size and shape, and appear less organized [1].

Despite the variations in mitochondrial size and shape in individual myocytes, very little is known about mitochondrial dynamics in the adult heart. Several recent studies show the presence of mitochondrial fission and fusion proteins in heart tissue, indicating that mitochondrial structure may be dynamic in the heart as well [3–7]. In addition, the high incidence of abnormal mitochondrial morphologies associated with many cardiac diseases suggests a role for these processes in normal cardiac function and abnormal disease etiology [8–14]. However, due to the highly organized and more static structure of the mitochondria in adult cardiac myocyte, it remains unclear whether these mitochondria are capable of undergoing fusion and fission and if mitochondrial dynamics plays a physiological role in the heart.

In many cell types, the dynamic interconversion between mitochondrial fusion and fission ***is*** important for normal cellular function. This becomes apparent as mutations or knockouts of the genes involved in mitochondrial dynamics have been shown to be lethal as well as cause human diseases [15–22]. Each process requires a different cohort of proteins. For example, mitochondrial fission requires the 17kD mitochondrial outer membrane protein, hFis1, and the recruitment of the 80–85kD large cytosolic GTPase DLP1 to the mitochondrial surface via transient interaction with hFis1 [23,24]. DLP1 is presumed to self-assemble into a homo-oligomeric ring around the mitochondrion [25] and possibly acts as a mechanoenzyme to pinch the mitochondrial membranes. GTP hydrolysis is required for the DLP1 constriction and disassembly, and a point mutation in this domain, such as DLP1-K38A, leads to a dominant negative fission-defective mutant and elongation of mitochondria due to reduced fission [26–29]. DLP1-K38A also has other effects on cellular physiology, such as changing the distribution and morphology of the endoplasmic reticulum (ER) [27].

In this study, we addressed the question of mitochondrial dynamics in the cardiac myocyte using thapsigargin (TG), a sarcoplasmic/endoplasmic reticulum Ca^{2+}-ATPase (SERCA) inhibitor, which has been previously shown to increase intracellular Ca^{2+} leading to mitochondrial fission via a DLP1-dependent process [30,31]. We demonstrated that not only does Ca^{2+} regulate a DLP1-dependent mitochondrial fission but also ROS production. These findings are the first evidence to indicate the role of Ca^{2+} regulation of mitochondrial fragmentation and ROS generation in cardiac muscle cells.

2. MATERIALS AND METHODS

2.1. Neonatal rat ventricular cardiomyocyte culture

As modified from a previously published procedure [32], the hearts from 1–3 day old anesthetized Sprague-Dawley rats were aeseptically removed and transferred to HBSS containing 0.1% BSA and rinsed. Ventricles were minced and digested in BSA-free HBSS, 0.5mg/mL collagenase (Worthington, type II) solution at 37°C. The cells were filtered, pelleted, and resuspended in DMEM with 50U/mL penicillin G, 10% calf serum, and 10% horse serum. Cells were pre-plated once for 30 min and again for 60 min. Cells unattached to

the plate were collected and plated on glass coverslips. After 24 hours the cultures were treated with 1:100 arabinosylcytosine (ara-C) for 48 hours to reduce the growth of fibroblasts. Cells were treated with fresh medium and used for experiments from day 5–7 in culture. In some cases, cells were transfected with a vector expressing either untagged or GFP-tagged mutant DLP1-K38A using FuGENE (Roche) according to manufacturer's instructions as described previously [27]. For treatments and visualization, untransfected (control) and transfected (GFP positive) cells were examined from the same specimen.

2.2. Isolation of adult rat ventricular myocytes

The procedure was described in a published paper [33].

2.3. Ca^{2+} imaging

Modified from the procedure published previously [34], cells were loaded with 7 μM Fura-2/AM and 0.02% Pluronic F-127 (Invitrogen) in HEPES buffer (10 mM HEPES, 10 mM glucose, 140 mM NaCl, 5 mM KCl, 1.8 mM $CaCl_2$, 2 mM $MgCl_2$, pH 7.4) at 37°C for 30 min to allow the dye to accumulate in the cytosol. Cells were washed for 30 min at 37°C to allow for de-esterification before experiments. After TG (Sigma-Aldrich, Co) addition, cells were sequentially excited at 340 nm and 380 nm, and cytosolic free Ca^{2+} was detected at 510 nm. Mitochondrial Ca^{2+} was measured by loading cells with 5 μM Rhod-2/AM (Invitrogen) at 4° C for 15 min to allow the dye to accumulate in the mitochondria, for 15 min at room temperature, and were washed for 15 min. Cells were incubated with 10 μM Ru360 for 30 min at room temperature to block mitochondrial Ca^{2+} uptake. All graphs were plotted as F/F_0 +/− SEM.

2.4. Fluorescence Imaging

Indirect immunofluorescence was performed as described previously [29,35]. Cells were fixed with 4% paraformaldehyde, permeabilized, and incubated in blocking buffer containing 5% horse serum for 1 hour at 37°C. Rabbit anti-DLP-N (described previously [36]) or mouse monoclonal anti-cytochrome c antibodies (Pharmingen), and Alexa 488 or 594-conjugated antibodies (Invitrogen) were used for primary and secondary antibodies, respectively. After appropriate washing, coverslips were mounted in ProLong antifade reagent (Invitrogen) on glass slides.

Live mitochondria were visualized by either loading with 200 nM Mitotracker Red CMXRos, or 5 μM MitoSOX Red (Invitrogen) in cultured neonatal ventricular myocytes at 37°C in HEPES buffer. With a 150W xenon lamp from the illumination unit polychrome [36]V, single cell images were taken by fluorescent microscopy (TILL Photonics LLC, Pleasanton, CA). The fluorescent imaging system uses a Nikon TE2000s inverted microscope with a 40× oil objective. Neonatal ventricular myocyte mitochondria were analyzed as described previously [31,37].

2.5. Mitochondrial Isolation

Cardiomyocytes were collected at 700 × g for 5 min at 4°C before and at various times after treatment with TG. The supernatant was discarded and the cell pellet was homogenized in 1 ml isolation buffer (10 mM HEPES pH 7.4, 1 mM EDTA, 320 mM sucrose, protease inhibitor). The homogenate was centrifuged at 700 × g for 8 min at 4°C and the supernatant was collected. The pellet was subjected to re-homogenization, centrifuged, and the supernatants were pooled. The supernatants were centrifuged at 17,000 × g for 11 min at 4°C and the supernatant (cytosol) and the pellet (mitochondria) were separated.

2.6. SDS-PAGE and Western Blotting

SDS-PAGE [38] and Western blotting was performed as described previously [36]. We used anti-DLP1-N [39], anti-Fis1 (Santa Cruz Biotechnology, Santa Cruz, CA), anti-GAPDH (Millipore, Billerica, MA), and anti-VDAC (Calbiochem, San Diego, CA) antibodies. Blots were developed with supersignal chemiluminescence detection substrate (Pierce, Rockford, IL).

2.7. Electron Microscopy

Specimens were prepared for and analyzed by electron microscopy at the University of Rochester Core Facility, as described previously [40]. Mitochondria from adult ventricular myocytes were analyzed using AnalySIS software (University of Rochester, Electron Microscope Core Facility) for form factor, aspect ratio, and area.

2.8. Statistical analysis

The data were statistically analyzed by parametric (two tailed t-test, one way analysis of variance with Dunnett's post-hoc testing) and non-parametric methods (Kruskal-Wallis with Dunn's post-hoc testing) using either Prism (GraphPad Software, La Jolla, CA) or SPSS (SPSS Inc., Chicago, IL). A P value < 0.05 was considered statistically significant.

2.9.Ethical Aspects

Due to the lack of appropriate cell lines for cardiomyocytes, it was necessary to isolate cardiac cells in primary culture from newborn rats and adult rats. The animals were kept in the University of Rochester vivarium and treated humanely. Each animal was sacrificed consistent with UCAR protocol 2006063 and the Panel of Euthanasia of the American Veterinary Medical Association.

3. RESULTS

Both adult and neonatal rat ventricular myocytes were used for experiments. Cultured neonatal rat ventricular myocytes were used for live cell imaging of mitochondrial morphology and function, taking advantage of their thin morphology with a lower density of mitochondria and relative ease of transfection. In contrast, in order to evaluate mitochondrial morphology in adult ventricular myocytes, electron microscopy was used because their thicker cell diameter with densely populated mitochondria limited the spatial resolution of optical microscopy.

3.1. Mitochondrial fission proteins are expressed in rat ventricular myocytes and respond to elevated Ca^{2+} concentrations

Mitochondrial fission requires the two proteins, hFis1 and DLP1. Western blotting showed that both hFis1 and DLP1 were expressed in myocytes at day 2 and 7 in culture (Fig. 1A). This indicates that cardiac mitochondria possess the components necessary to undergo fission events, in agreement with the previous identification of DLP1 mRNA in adult human heart [6].

TG is known to cause a global increase of cytosolic Ca^{2+} concentrations by inhibiting Ca^{2+} uptake at the SR/ER via SERCA [41]. In addition, TG has been shown to cause mitochondrial fragmentation via enhanced mitochondrial Ca^{2+} uptake [31]. Therefore, we used TG to examine whether mitochondria are able to undergo Ca^{2+} induced fragmentation in cardiac myocytes. Ca^{2+} imaging using Fura-2 showed that addition of 1 μM TG to cultured neonatal rat ventricular myocytes induced an immediate increase of cytosolic Ca^{2+} which gradually decreased to approximately half the peak by 10 min (Fig. 1B, left). Similar effects on cytosolic Ca^{2+} were observed after treatment with 50 mM KCl, which opens L-type Ca^{2+} channels via

membrane depolarization (Fig. 1B, left). Mitochondrial Ca^{2+} imaging using Rhod-2 demonstrated that TG also induced a rise in mitochondrial free Ca^{2+}, which could be blocked by preincubation with 10 μM Ru360, which inhibits mitochondrial Ca^{2+} uptake (Fig. 1B, right). Similar effects of TG were observed in adult rat ventricular myocytes (data not shown).

DLP1 translocation from the cytosol to mitochondria is an early step in mitochondrial fission [15,16,26]. We next assessed whether TG induced DLP1 translocation to mitochondria in isolated adult cardiac myocytes. This preparation provides a larger quantity of proteins than neonatal heart cells for such experiments. Freshly isolated adult rat cardiac myocytes were treated with 1 μM TG for 5, 10, 30, and 60 min, and the mitochondrial fraction was collected and examined for the presence of DLP1 by Western blot. TG caused an accumulation of DLP1 in the mitochondrial fraction at 5, 10, and 30 min compared to controls (Fig. 1C). However, after 60 min of treatment with TG, DLP1 returned to similar levels as controls, indicating that the TG-induced DLP1 translocation was a transient event (Fig. 1C). The time course of elevated Ca^{2+} levels and DLP1 accumulation in the mitochondrial fraction was similar suggesting that TG induced DLP1 accumulation via elevated Ca^{2+} levels. These results indicate that increased cytosolic Ca^{2+} in adult cardiac myocytes induces DLP1 translocation to mitochondria, an early event of mitochondrial fission. We obtained similar results treating cells with 50 mM KCl (data not shown).

3.2. TG induces a rapid change in mitochondrial morphology in neonatal and adult cardiac myocytes

Next, we tested the effects of TG-induced cytosolic Ca^{2+} increase on mitochondrial morphology in rat neonatal ventricular myocytes. These myocytes normally displayed filamentous or tubular mitochondria along with large, globular mitochondria that were often continuous with mitochondrial tubules. We observed a rapid change in mitochondrial morphology upon invoking an increase in cytosolic Ca^{2+} with either 1 μM TG or 50 mM KCl. While mitochondria from untreated cells displayed normal tubular/globular morphology (Fig. 2A, control), within 5 min after the addition of TG or KCl, the tubular and globular mitochondria became small and punctate, indicating mitochondrial fragmentation (Fig. 2A and 3C). Furthermore, inhibition of mitochondrial Ca^{2+} uptake with Ru360 prevented mitochondrial fragmentation in TG-treated cells, suggesting that mitochondrial Ca^{2+} uptake is necessary for mitochondrial fragmentation (Fig. 2A).

To test if mitochondrial fragmentation could occur in adult cardiac myocytes, freshly isolated adult rat ventricular myocytes were treated with 1 μM TG for 5, 10, or 30 min, and immediately fixed and prepared for electron microscopy and morphometric analysis (Fig. 2B and C). We measured area, perimeter, and major and minor axes for individual mitochondria within single cells (2 experiments, 10 cells per time point). Analysis of mitochondrial area revealed that control cardiac muscle contained a wide range of mitochondrial sizes (mean = 0.372 μm^2, range 0.039 to 0.873 μm^2) with a non-Gaussian distribution. Therefore, a non-parametric analysis of area was performed. At 5 min TG treatment, mitochondrial area was significantly smaller than controls (mean = 0.189 μm^2, range 0.007 to 0.833 μm^2). At 10 and 30 min TG treatment, mitochondrial area had largely recovered to control values, although the range of areas remained wider (10 min: mean = 0.324 μm^2, range 0.016 to 1.149 μm^2 ; 30 min: mean = 0.360 μm^2, range 0.020 to 0.892 μm^2). A histogram of the frequency distribution of the area demonstrates these changes in mitochondrial area and suggests that TG induces an immediate (5 min) fragmentation of most mitochondria (Fig. 2C). At 10 and 30 min, mitochondria appeared to be recovering from this fragmentation.

We also measured aspect ratio (AR; major axis/minor axis), which is a measure of mitochondrial length, and form factor (FF; $perimeter^2/4\pi \cdot Area$), which is a measure of mitochondrial length and branching [37]. AR and FF both have a minimum value of 1 when

the mitochondrion is a small, perfect circle, and these values increase as the mitochondrion becomes elongated and/or branched. During the time course of TG treatment, the FF was significantly decreased at 5 min compared to 0, 10, and 30 min TG, indicating that the mitochondria tended to be more fragmented and less branched (Fig. 2D). The values of FF at 10 and 30 min TG were similar to 0 min, indicating recovery of mitochondrial morphology. Analysis of AR revealed a trend toward shorter mitochondria after 5 min TG that was not statistically significant. However, at 10 min TG, mitochondria were significantly longer compared to 5 min TG, indicating that as the mitochondrial morphology recovered after fragmentation (Fig. 2D).

3.3. TG-induced mitochondrial fragmentation in cardiac myocytes requires the mitochondrial fission protein DLP1

To test whether TG induces the normal mitochondrial fission process, neonatal rat ventricular myocytes were transfected with dominant negative DLP1-K38A, and mitochondrial morphology was assessed before and after TG treatment. Control cells showed a cytoplasmic distribution of DLP1 and a mixture of elongated and large globular mitochondria with only a slight colocalization between the DLP1 and mitochondria (Fig. 3A). In contrast, overexpression of DLP1-K38A (detected with anti-DLP1 antibodies) caused the elongation of mitochondrial tubules that formed an interconnected network. Also, characteristic of dominant negative DLP1-K38A overexpression were the accumulations of large cytosolic DLP1 aggregates, which has been reported in previous studies [26–29,31,35] (Fig. 3B). Little colocalization between DLP1 and mitochondria was observed in the DLP1-K38A overexpressing cells (Fig. 3B).

When GFP-tagged DLP1-K38A overexpressing cells were treated with TG, the mitochondria in these cells remained elongated tubules, whereas untransfected (UT) cells from the same dish underwent drastic fragmentation of mitochondria after 5 min (Fig. 3C). Therefore, mutant DLP1 disrupted normal mitochondrial fission in neonatal myocytes and prevented TG-induced mitochondrial fragmentation. These data demonstrate that increased cytosolic Ca^{2+} may act upstream of the DLP1 scission enzyme to activate the cellular mitochondrial fission machinery.

3.4. Superoxide generation with TG coincides with mitochondrial fragmentation in neonatal ventricular myocytes

An increase in mitochondrial Ca^{2+} can increase ROS generation by several mechanisms, including mitochondrial fission [42,43]. Therefore, we examined the link between TG-induced cytosolic Ca^{2+} increase, mitochondrial fragmentation, and ROS generation. To test the effects of TG on ROS production, we performed MitoSOX Red imaging using neonatal myocytes with and without transfection with DLP1-K38A. Upon the addition of 1 μM TG to control cells, ROS production increased by approximately 70% (Fig. 4A). Addition of 10 μM antimycin A, a complex III inhibitor, induced maximum superoxide production. In contrast, overexpression of DLP1-K38A significantly attenuated the TG-induced superoxide increase, as the superoxide only increased by approximately 20% (Fig. 4A). Figure 4B shows the summarized results. The block of TG-induced superoxide increase due to DLP1-K38A overexpression suggests that DLP1 (mitochondrial fission) is necessary for TG-induced superoxide increase. These data may also indicate that Ca^{2+}-induced mitochondrial fission occurs upstream of ROS production.

4. DISCUSSION

4.1. Ca^{2+} signals regulate cardiac mitochondrial morphology

Despite the presence of mitochondrial fission proteins in the heart, there is currently very little evidence that cardiac mitochondria undergo fragmentation. In addition, elevated levels of

cytosolic Ca^{2+} are known to induce mitochondrial fragmentation in various cell types [31]. Since cardiac myocytes depend on large cyclic changes in Ca^{2+}, we tested whether mitochondria from these cells undergo fragmentation and if this process is regulated by Ca^{2+} and contributes to Ca^{2+}-mediated mitochondrial ROS generation.

Using fluorescence imaging techniques, we observed that in neonatal ventricular myocytes, TG or high KCl induced a change from normal globular and tubular mitochondria to small, round, punctate mitochondria, indicating that mitochondria in immature myocytes can undergo fragmentation in response to Ca^{2+} signals. Because of the limitations in observing specific changes in adult cardiac mitochondrial morphology using fluorescence microscopy, we used electron microscopy to determine whether similar changes occur in adult mitochondria. Electron micrographs revealed that the increased cytosolic Ca^{2+} induced by TG also caused a reversible mitochondrial fragmentation in adult cardiac myocytes, which had smaller area, FF, and AR at 5 min after treatment. After the mitochondrial fragmentation at 5 min, however, the presence of the very large mitochondria observed at 10 min may indicate not only a recovery of normal mitochondrial morphology, but an “overshoot” of mitochondrial fusion in response to the excessive mitochondrial fission as observed previously [31]. These results are among the first to show that mature cardiac myocytes undergo fragmentation and demonstrate that this process is under the control of intracellular Ca^{2+} levels.

We acknowledge some limitations to these analyses of mitochondrial morphology in adult cardiac myocytes. Although our morphometry data indicate changes in mitochondrial morphology, 70 nm sections of electron micrograph do not reveal the extended structure of an individual mitochondrion. Perhaps future experiments using 3-dimensional reconstruction of confocal or EM data will better define global changes in mitochondrial morphology induced by elevated Ca^{2+}.

TG is known to have other side effects on cellular physiology due to prolonged depletion of ER/SR Ca^{2+}, which leads to the misfolding of proteins, activation of caspases, and cell death [44,45]. Mitochondrial fragmentation is also associated with apoptosis and therefore it is important to consider whether our TG incubations cause pathological fragmentation of mitochondria. In our previous study, Clone 9 cells underwent rapid fragmentation of mitochondria during the first 60 minute exposure to TG without evidence of cell death. Only after 32 hours of prolonged exposure to TG, apoptosis-associated mitochondrial fragmentation was observed [31]. We found a similar reversal of mitochondrial fragmentation and no overt evidence of cell death in cardiac myocytes treated for 60 min with TG. Therefore, it is unlikely that the mitochondrial fragmentation we observed in our experiments was associated with apoptosis from prolonged exposure to TG.

4.2. Ca^{2+}-induced mitochondrial fragmentation involves DLP1

We next tested if TG-induced mitochondrial fragmentation in cardiac myocytes requires the known mitochondrial fission process which involves translocation of cytoplasmic DLP1 to mitochondria. We observed that in adult cardiac myocytes, TG treatment caused DLP1 translocation from the cytosol to the mitochondria, an early step in mitochondrial fission. Interestingly, DLP1 remained on the mitochondria up to 30 minutes after TG treatment, but mitochondrial fragmentation reversed as early as 10 minutes after TG treatment. Previous evidence that endogenous DLP1 remains bound to mitochondria after fission events have occurred may explain this phenomenon [28]. In addition, we found that DLP1-K38A expression causes the mitochondria to form elongated tubules which, unlike in untransfected cells, did not fragment upon TG treatment. Together, these data suggest that the mechanism of Ca^{2+} dependent mitochondrial fragmentation in cardiac myocytes involves the known fission machinery.

What are the mechanisms by which an increase in intracellular Ca^{2+} leads to the activation of the mitochondrial fission machinery? There may be both mitochondrial and cytosolic pathways that activate hFis1 and DLP1. Some data suggest that mitochondrial Ca^{2+} uptake is necessary for mitochondrial fragmentation in different cell types [31,46]. This agrees with our Ru360 results, which effectively blocked TG-induced mitochondrial Ca^{2+} uptake and fragmentation in cultured neonatal ventricular myocytes. It may be possible that hFis1, which has been shown to regulate DLP1 recruitment and assembly, may interact with inner mitochondrial proteins or membrane spanning protein complexes that are regulated by Ca^{2+}. However, Ca^{2+} signaling pathways in the cytosol have been shown to regulate mitochondrial morphology via phosphorylation and dephosphorylation of DLP1 [47–52]. Future experiments will be necessary to elucidate how mitochondrial Ca^{2} increase activates the mitochondrial fission machinery, and if this is a different pathway than DLP1 activation.

4.3. Ca^{2+} induction of ROS generation involves mitochondrial fragmentation

We then tested the role of Ca^{2+}-induced mitochondrial fragmentation and DLP1 on ROS generation, which reflects mitochondrial respiration as well as pathology. We found that TG caused an increase in intracellular Ca^{2+} followed by mitochondrial fragmentation and an increase in ROS. DLP1 appears to be involved in this, as our data indicate that inhibiting fission with DLP1-K38A abated a rise in ROS. This suggests that the increase in ROS is not immediately downstream of increased intracellular Ca^{2+}, and that DLP1 and/or mitochondrial fragmentation contribute to the TG-induced ROS increase. It remains unknown whether the mitochondrial fission-mediated and electron transport chain (ETC)-mediated ROS generating mechanisms are separate and additive, or if DLP1 plays a role in modulating ETC-mediated ROS generation, as has been suggested previously [41]. On one hand, the effects of TG and ETC-mediated ROS generation could be additive, as the absolute rise in ROS after antimycin A is approximately the same in both the untreated and the DLP1-K38A cells (Fig. 4A). Interestingly, our preliminary evidence suggests that DLP1 may play a role in modulating the ROS generation from the ETC (Yoon, unpublished observations). It should also be noted that our experiments showing that the rate of antimycin A-induced ROS increase was slower in DLP1-K38A cells (Figure 4A), may also suggest this interaction. In addition, these treatments may have induced a pathologic state, in which mitochondria produce ROS associated with the mitochondrial permeability transition pore (mPTP) opening. However, as discussed above, our previous results suggest that short term TG exposure does not induce these pathologic changes. Finally, these treatments may induce a nonpathological opening of the mPTP involving superoxide flashes [53]. Future experiments with the measurements of mitochondrial membrane potential in the presence and absence of blockers for mPTP will be useful to resolve these probable mechanisms.

5. CONCLUSIONS

In conclusion, we tested the role of Ca^{2+} in controlling mitochondrial morphology in cardiac myocytes and provide some of the first evidence that mitochondrial fragmentation occurs in neonatal and adult cardiac myocytes. This dynamic change in mitochondrial shape is linked to the functional activity of the mitochondria, as TG increased superoxide production. In addition, these Ca^{2+} dependent changes in mitochondrial structure and function were mediated by the fission protein DLP1. This indicates that Ca^{2+} is one common factor that regulates both cardiac mitochondrial form and function in the heart.

Acknowledgments

We gratefully acknowledge support from National Institutes of Health Grants DK 61991, DK 73858 and HL 33333. We thank Karen Bentley and the University of Rochester Electron Microscope core, Gisela Beutner, Donna DiManno,

and Virendra Sharma who provided help during the research, and discussions with the members of Mitochondrial Research & Innovation Group.

REFERENCES

1. Hom J, Sheu SS. Morphological dynamics of mitochondria--a special emphasis on cardiac muscle cells. J Mol Cell Cardiol 2009;46:811–820. [PubMed: 19281816]
2. Sharma VK, Ramesh V, Franzini-Armstrong C, Sheu SS. Transport of Ca2+ from sarcoplasmic reticulum to mitochondria in rat ventricular myocytes. J Bioenerg Biomembr 2000;32:97–104. [PubMed: 11768767]
3. Santel A, Frank S, Gaume B, Herrler M, Youle RJ, Fuller MT. Mitofusin-1 protein is a generally expressed mediator of mitochondrial fusion in mammalian cells. J Cell Sci 2003;116:2763–2774. [PubMed: 12759376]
4. Rojo M, Legros F, Chateau D, Lombes A. Membrane topology and mitochondrial targeting of mitofusins, ubiquitous mammalian homologs of the transmembrane GTPase Fzo. J Cell Sci 2002;115:1663–1674. [PubMed: 11950885]
5. Bach D, Pich S, Soriano FX, Vega N, Baumgartner B, Oriola J, Daugaard JR, Lloberas J, Camps M, Zierath JR, Rabasa-Lhoret R, Wallberg-Henriksson H, Laville M, Palacin M, Vidal H, Rivera F, Brand M, Zorzano A. Mitofusin-2 determines mitochondrial network architecture and mitochondrial metabolism. A novel regulatory mechanism altered in obesity. J Biol Chem 2003;278:17190–17197. [PubMed: 12598526]
6. Imoto M, Tachibana I, Urrutia R. Identification and functional characterization of a novel human protein highly related to the yeast dynamin-like GTPase Vps1p. J Cell Sci 1998;111(Pt 10):1341–1349. [PubMed: 9570752]
7. Akepati VR, Muller EC, Otto A, Strauss HM, Portwich M, Alexander C. Characterization of OPA1 isoforms isolated from mouse tissues. J Neurochem 2008;106:372–383. [PubMed: 18419770]
8. Schaper J, Froede R, Hein S, Buck A, Hashizume H, Speiser B, Friedl A, Bleese N. Impairment of the myocardial ultrastructure and changes of the cytoskeleton in dilated cardiomyopathy. Circulation 1991;83:504–514. [PubMed: 1991369]
9. Scholz D, Diener W, Schaper J. Altered nucleus/cytoplasm relationship and degenerative structural changes in human dilated cardiomyopathy. Cardioscience 1994;5:127–138. [PubMed: 7919049]
10. Ausma J, Thone F, Dispersyn GD, Flameng W, Vanoverschelde JL, Ramaekers FC, Borgers M. Dedifferentiated cardiomyocytes from chronic hibernating myocardium are ischemia-tolerant. Mol Cell Biochem 1998;186:159–168. [PubMed: 9774197]
11. Kalra DK, Zoghbi WA. Myocardial hibernation in coronary artery disease. Curr Atheroscler Rep 2002;4:149–155. [PubMed: 11822979]
12. Trillo AA, Holleman IL, White JT. Presence of satellite cells in a cardiac rhabdomyoma. Histopathology 1978;2:215–223. [PubMed: 669594]
13. Jones M, Ferrans VJ, Morrow AG, Roberts WC. Ultrastructure of crista supraventricularis muscle in patients with congenital heart diseases associated with right ventricular outflow tract obstruction. Circulation 1975;51:39–67. [PubMed: 122789]
14. Terman A, Dalen H, Eaton JW, Neuzil J, Brunk UT. Aging of cardiac myocytes in culture: oxidative stress, lipofuscin accumulation, and mitochondrial turnover. Ann N Y Acad Sci 2004;1019:70–77. [PubMed: 15246997]
15. Waterham HR, Koster J, van Roermund CW, Mooyer PA, Wanders RJ, Leonard JV. A lethal defect of mitochondrial and peroxisomal fission. N Engl J Med 2007;356:1736–1741. [PubMed: 17460227]
16. Labrousse AM, Zappaterra MD, Rube DA, van der Bliek AM. C. elegans dynamin-related protein DRP-1 controls severing of the mitochondrial outer membrane. Mol Cell 1999;4:815–826. [PubMed: 10619028]
17. Chen H, Detmer SA, Ewald AJ, Griffin EE, Fraser SE, Chan DC. Mitofusins Mfn1 and Mfn2 coordinately regulate mitochondrial fusion and are essential for embryonic development. J Cell Biol 2003;160:189–200. [PubMed: 12527753]
18. Chen H, Chomyn A, Chan DC. Disruption of fusion results in mitochondrial heterogeneity and dysfunction. J Biol Chem 2005;280:26185–26192. [PubMed: 15899901]

19. Pareyson D. Differential diagnosis of Charcot-Marie-Tooth disease and related neuropathies. Neurol Sci 2004;25:72–82. [PubMed: 15221625]
20. Zuchner S, Mersiyanova IV, Muglia M, Bissar-Tadmouri N, Rochelle J, Dadali EL, Zappia M, Nelis E, Patitucci A, Senderek J, Parman Y, Evgrafov O, Jonghe PD, Takahashi Y, Tsuji S, Pericak-Vance MA, Quattrone A, Battaloglu E, Polyakov AV, Timmerman V, Schroder JM, Vance JM. Mutations in the mitochondrial GTPase mitofusin 2 cause Charcot-Marie-Tooth neuropathy type 2A. Nat Genet 2004;36:449–451. [PubMed: 15064763]
21. Alexander C, Votruba M, Pesch UE, Thiselton DL, Mayer S, Moore A, Rodriguez M, Kellner U, Leo-Kottler B, Auburger G, Bhattacharya SS, Wissinger B. OPA1, encoding a dynamin-related GTPase, is mutated in autosomal dominant optic atrophy linked to chromosome 3q28. Nat Genet 2000;26:211–215. [PubMed: 11017080]
22. Delettre C, Lenaers G, Griffoin JM, Gigarel N, Lorenzo C, Belenguer P, Pelloquin L, Grosgeorge J, Turc-Carel C, Perret E, Astarie-Dequeker C, Lasquellec L, Arnaud B, Ducommun B, Kaplan J, Hamel CP. Nuclear gene OPA1, encoding a mitochondrial dynamin-related protein, is mutated in dominant optic atrophy. Nat Genet 2000;26:207–210. [PubMed: 11017079]
23. Yoon Y, Krueger EW, Oswald BJ, McNiven MA. The mitochondrial protein hFis1 regulates mitochondrial fission in mammalian cells through an interaction with the dynamin-like protein DLP1. Mol Cell Biol 2003;23:5409–5420. [PubMed: 12861026]
24. Yu T, Fox RJ, Burwell LS, Yoon Y. Regulation of mitochondrial fission and apoptosis by the mitochondrial outer membrane protein hFis1. J Cell Sci 2005;118:4141–4151. [PubMed: 16118244]
25. Ingerman E, Perkins EM, Marino M, Mears JA, McCaffery JM, Hinshaw JE, Nunnari J. Dnm1 forms spirals that are structurally tailored to fit mitochondria. J Cell Biol 2005;170:1021–1027. [PubMed: 16186251]
26. Smirnova E, Shurland DL, Ryazantsev SN, van der Bliek AM. A human dynamin-related protein controls the distribution of mitochondria. J Cell Biol 1998;143:351–358. [PubMed: 9786947]
27. Pitts KR, Yoon Y, Krueger EW, McNiven MA. The dynamin-like protein DLP1 is essential for normal distribution and morphology of the endoplasmic reticulum and mitochondria in mammalian cells. Mol Biol Cell 1999;10:4403–4417. [PubMed: 10588666]
28. Smirnova E, Griparic L, Shurland DL, van der Bliek AM. Dynamin-related protein Drp1 is required for mitochondrial division in mammalian cells. Mol Biol Cell 2001;12:2245–2256. [PubMed: 11514614]
29. Yoon Y, Pitts KR, McNiven MA. Mammalian dynamin-like protein DLP1 tubulates membranes. Mol Biol Cell 2001;12:2894–2905. [PubMed: 11553726]
30. Thastrup O, Cullen PJ, Drobak BK, Hanley MR, Dawson AP. Thapsigargin, a tumor promoter, discharges intracellular Ca2+ stores by specific inhibition of the endoplasmic reticulum Ca2(+)-ATPase. Proc Natl Acad Sci U S A 1990;87:2466–2470. [PubMed: 2138778]
31. Hom JR, Gewandter JS, Michael L, Sheu SS, Yoon Y. Thapsigargin induces biphasic fragmentation of mitochondria through calcium-mediated mitochondrial fission and apoptosis. J Cell Physiol 2007;212:498–508. [PubMed: 17443673]
32. Colecraft HM, Egamino JP, Sharma VK, Sheu SS. Signaling mechanisms underlying muscarinic receptor-mediated increase in contraction rate in cultured heart cells. J Biol Chem 1998;273:32158–32166. [PubMed: 9822693]
33. Sheu SS, Sharma VK, Banerjee SP. Measurement of cytosolic free calcium concentration in isolated rat ventricular myocytes with quin 2. Circ Res 1984;55:830–834. [PubMed: 6499138]
34. Sharma VK, Colecraft HM, Wang DX, Levey AI, Grigorenko EV, Yeh HH, Sheu SS. Molecular and functional identification of m1 muscarinic acetylcholine receptors in rat ventricular myocytes. Circ Res 1996;79:86–93. [PubMed: 8925573]
35. Yu T, Robotham JL, Yoon Y. Increased production of reactive oxygen species in hyperglycemic conditions requires dynamic change of mitochondrial morphology. Proc Natl Acad Sci U S A 2006;103:2653–2658. [PubMed: 16477035]
36. Henley JR, McNiven MA. Association of a dynamin-like protein with the Golgi apparatus in mammalian cells. J Cell Biol 1996;133:761–775. [PubMed: 8666662]
37. Koopman WJ, Verkaart S, Visch HJ, van der Westhuizen FH, Murphy MP, van den Heuvel LW, Smeitink JA, Willems PH. Inhibition of complex I of the electron transport chain causes O2−. -

mediated mitochondrial outgrowth. Am J Physiol Cell Physiol 2005;288:C1440–C1450. [PubMed: 15647387]

38. Laemmli UK. Cleavage of structural proteins during the assembly of the head of bacteriophage T4. Nature 1970;227:680–685. [PubMed: 5432063]
39. Yoon Y, Pitts KR, Dahan S, McNiven MA. A novel dynamin-like protein associates with cytoplasmic vesicles and tubules of the endoplasmic reticulum in mammalian cells. J Cell Biol 1998;140:779–793. [PubMed: 9472031]
40. Lantum HB, Baggs RB, Krenitsky DM, Anders MW. Nephrotoxicity of chlorofluoroacetic acid in rats. Toxicol Sci 2002;70:261–268. [PubMed: 12441371]
41. Treiman M, Caspersen C, Christensen SB. A tool coming of age: thapsigargin as an inhibitor of sarco-endoplasmic reticulum Ca(2+)-ATPases. Trends Pharmacol Sci 1998;1:131–135. [PubMed: 9612087]
42. Brookes PS, Yoon Y, Robotham JL, Anders MW, Sheu SS. Calcium, ATP, and ROS a mitochondrial love-hate triangle. Am J Physiol Cell Physiol 2004;287:C817–C833. [PubMed: 15355853]
43. Yu T, Sheu SS, Robotham JL, Yoon Y. Mitochondrial fission mediates high glucose-induced cell death through elevated production of reactive oxygen species. Cardiovasc Res 2008;79:341–351. [PubMed: 18440987]
44. Kaneko Y, Tsukamoto A. Thapsigargin-induced persistent intracellular calcium pool depletion and apoptosis in human hepatoma cells. Cancer Lett 1994;79:147–155. [PubMed: 8019972]
45. Jiang S, Chow SC, Nicotera P, Orrenius S. Intracellular Ca2+ signals activate apoptosis in thymocytes: studies using the Ca(2+)-ATPase inhibitor thapsigargin. Exp Cell Res 1994;212:84–92. [PubMed: 8174645]
46. Breckenridge DG, Stojanovic M, Marcellus RC, Shore GC. Caspase cleavage product of BAP31 induces mitochondrial fission through endoplasmic reticulum calcium signals, enhancing cytochrome c release to the cytosol. J Cell Biol 2003;160:1115–1127. [PubMed: 12668660]
47. Han XJ, Lu YF, Li SA, Tomizawa K, Takei K, Matsushita M, Matsui H. Involvement of calcineurin in glutamate-induced mitochondrial dynamics in neurons. Neurosci Res 2008;60:114–119. [PubMed: 18045716]
48. Harder Z, Zunino R, McBride H. Sumo1 conjugates mitochondrial substrates and participates in mitochondrial fission. Curr Biol 2004;14:340–345. [PubMed: 14972687]
49. Nakamura N, Kimura Y, Tokuda M, Honda S, Hirose S. MARCH-V is a novel mitofusin 2- and Drp1-binding protein able to change mitochondrial morphology. EMBO Rep 2006;7:1019–1022. [PubMed: 16936636]
50. Taguchi N, Ishihara N, Jofuku A, Oka T, Mihara K. Mitotic phosphorylation of dynamin-related GTPase Drp1 participates in mitochondrial fission. J Biol Chem 2007;282:11521–11529. [PubMed: 17301055]
51. Chang CR, Blackstone C. Cyclic AMP-dependent protein kinase phosphorylation of Drp1 regulates its GTPase activity and mitochondrial morphology. J Biol Chem 2007;282:21583–21587. [PubMed: 17553808]
52. Cribbs JT, Strack S. Reversible phosphorylation of Drp1 by cyclic AMP-dependent protein kinase and calcineurin regulates mitochondrial fission and cell death. EMBO Rep 2007;8:939–944. [PubMed: 17721437]
53. Wang W, Fang H, Groom L, Cheng A, Zhang W, Liu J, Wang X, Li K, Han P, Zheng M, Yin J, Mattson MP, Kao JP, Lakatta EG, Sheu SS, Ouyang K, Chen J, Dirksen RT, Cheng H. Superoxide flashes in single mitochondria. Cell 2008;134:279–290. [PubMed: 18662543]

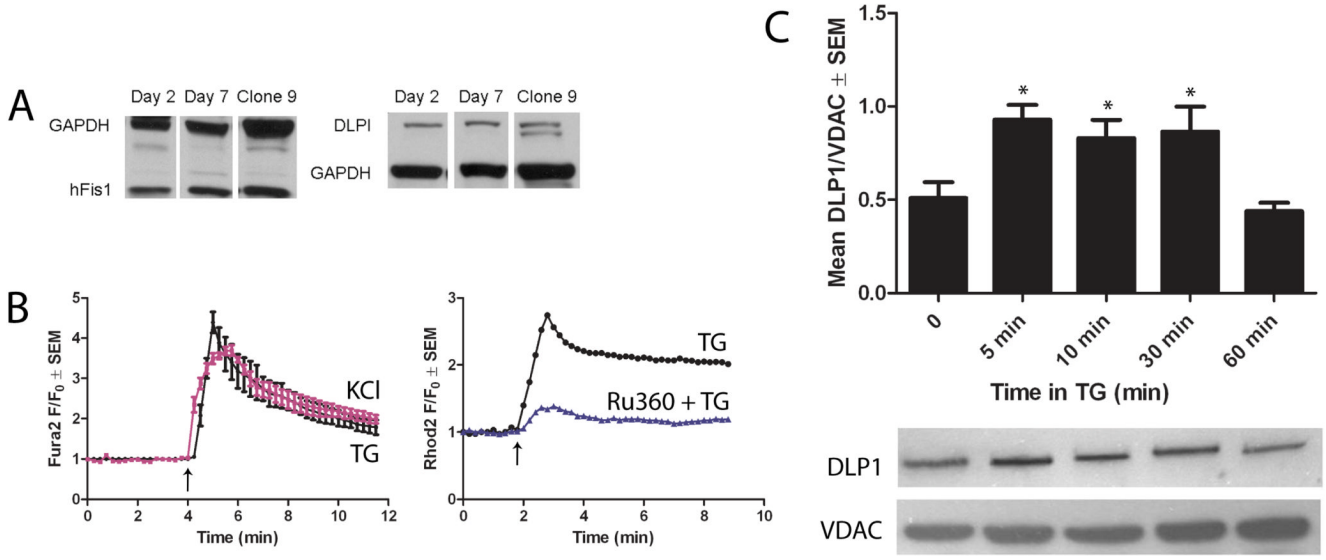

Figure 1. Ventricular myocytes express DLP1, which translocates to mitochondria upon TG-induced increase of cytosolic Ca^{2+}

(A) Western blotting demonstrates that neonatal rat ventricular myocytes endogenously express hFis1 and DLP1 from days 2–7 in culture. Clone 9 cells were used as a positive control for fission protein expression [23]. GAPDH was used as a loading control. (B) Ca^{2+} imaging using Fura-2 showed that either 1 μM TG (black line) or 50 mM KCl (pink line) induced an increase in cytosolic Ca^{2+}. The Fura-2 ratio (F_{340}/F_{360}) at each time point (F) was normalized against the initial ratio (F_0) for comparison (n=4). Representative traces of mitochondrial Ca^{2+} imaging using Rhod-2 showed that 1 μM TG (black line) induced mitochondrial Ca^{2+} uptake. Treatment with Ru360 (blue line) decreased mitochondrial Ca^{2+} uptake upon TG addition. (n=3) (C) Cultured adult cardiomyocytes were treated with 1 μM TG for 5, 10, 30, or 60 min and the mitochondrial fractions were isolated and assayed for DLP1 and VDAC (loading control) by Western blot. DLP1 association with mitochondria increased after 5, 10, and 30 min of TG treatment but returned to basal levels at 60 min TG (* P<0.01 by ANOVA with Dunnett's post-hoc test, n=4).

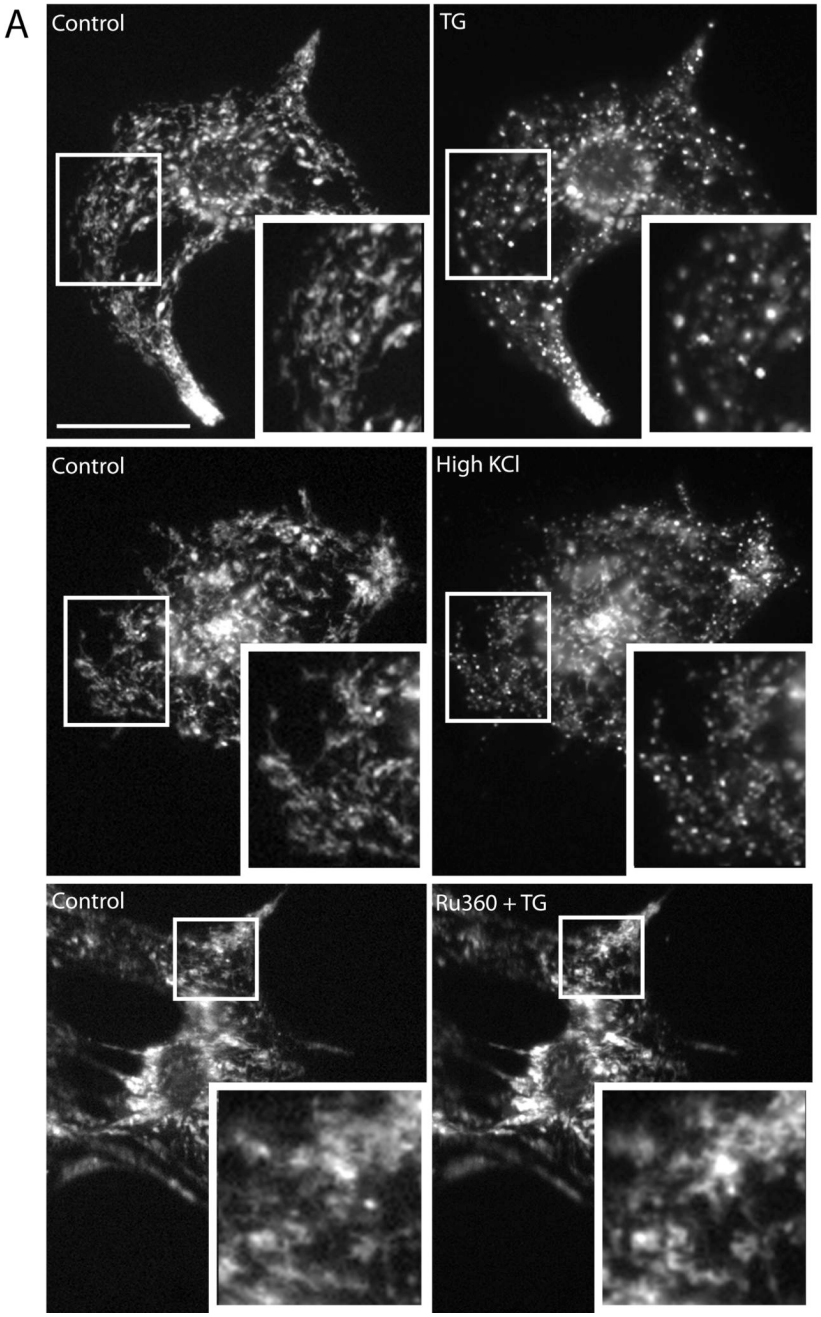

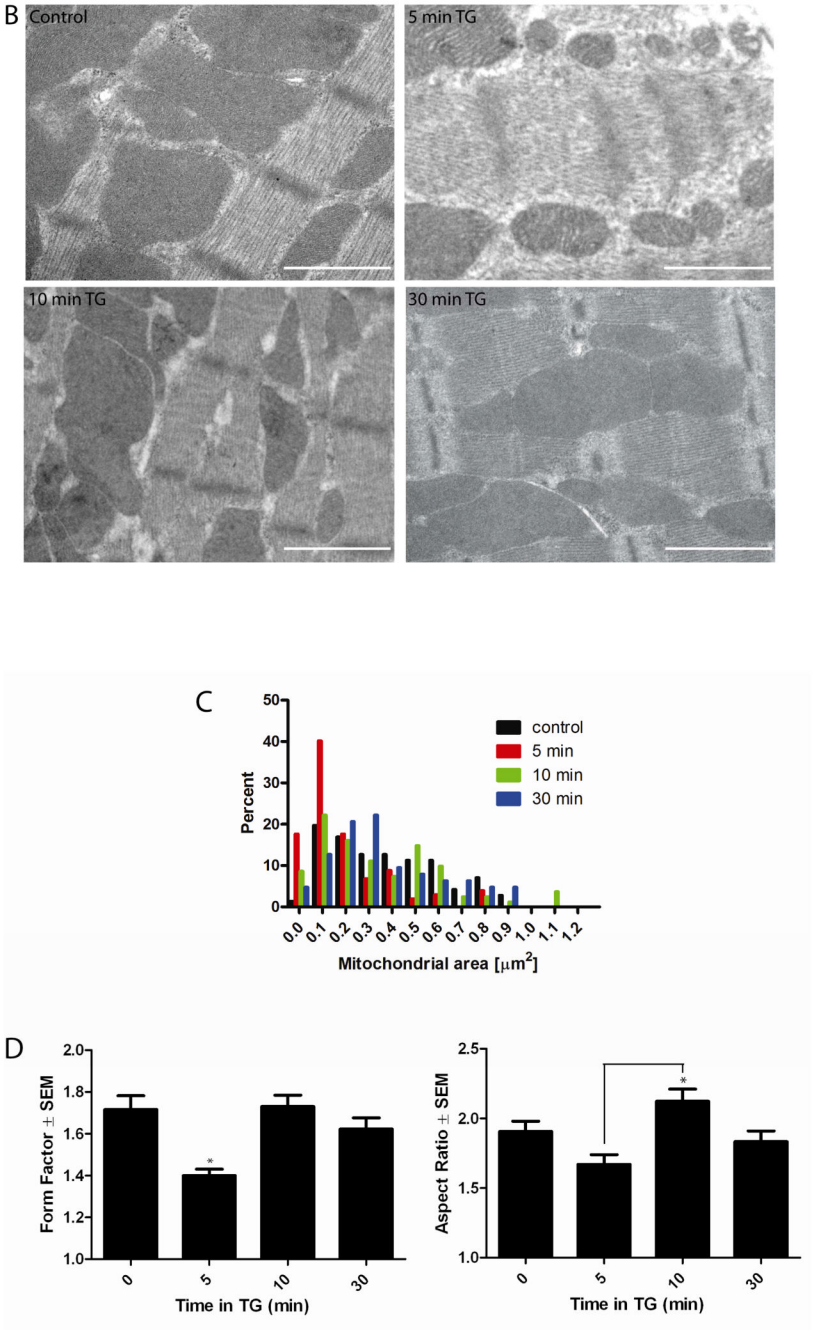

Figure 2. TG fragments mitochondria in neonatal and adult ventricular myocytes

(A) Within 5 min, either 1 μM TG or 50 mM KCl, induced mitochondrial fragmentation, compared to baseline, in cultured neonatal myocytes. Untreated cells displayed normal globular and tubular mitochondrial morphology (A, control). Preincubation with 10 μM Ru360 for 30 min and throughout the experiment inhibited TG-induced mitochondrial fragmentation at 5 min. Mitochondria were visualized using Mitotracker Red CMXRos. Scale bar = 30 μm. (B) Cultured adult cardiac myocytes were treated with 1 μM TG for 5, 10, and 30 min, fixed, and viewed under electron microscope. Cardiac mitochondria display various morphologies in control and at each time point but mitochondria appeared smaller and more fragmented at 5 min TG. Scale bar = 1 μm. (C) Consistent with this observation, a histogram of mitochondrial

area demonstrated a smaller mean mitochondrial area at 5 min TG, which recovered at 10 and 30 min TG compared to control. (D) Analysis of mitochondrial form factor demonstrates a decrease in mitochondrial branching and length from cells after 5 min of TG treatment compared to 0, 10, and 30 min TG, and a recovery of normal morphology at 10 and 30 min TG. Analysis of mitochondrial aspect ratio demonstrates shorter mitochondria at 5 min TG, with significant lengthening between 5 and 10 min followed by a return to baseline. (for all analyses, $*P<0.05$ using Kruskal-Wallis non-parametric testing with Dunn's post-hoc test)

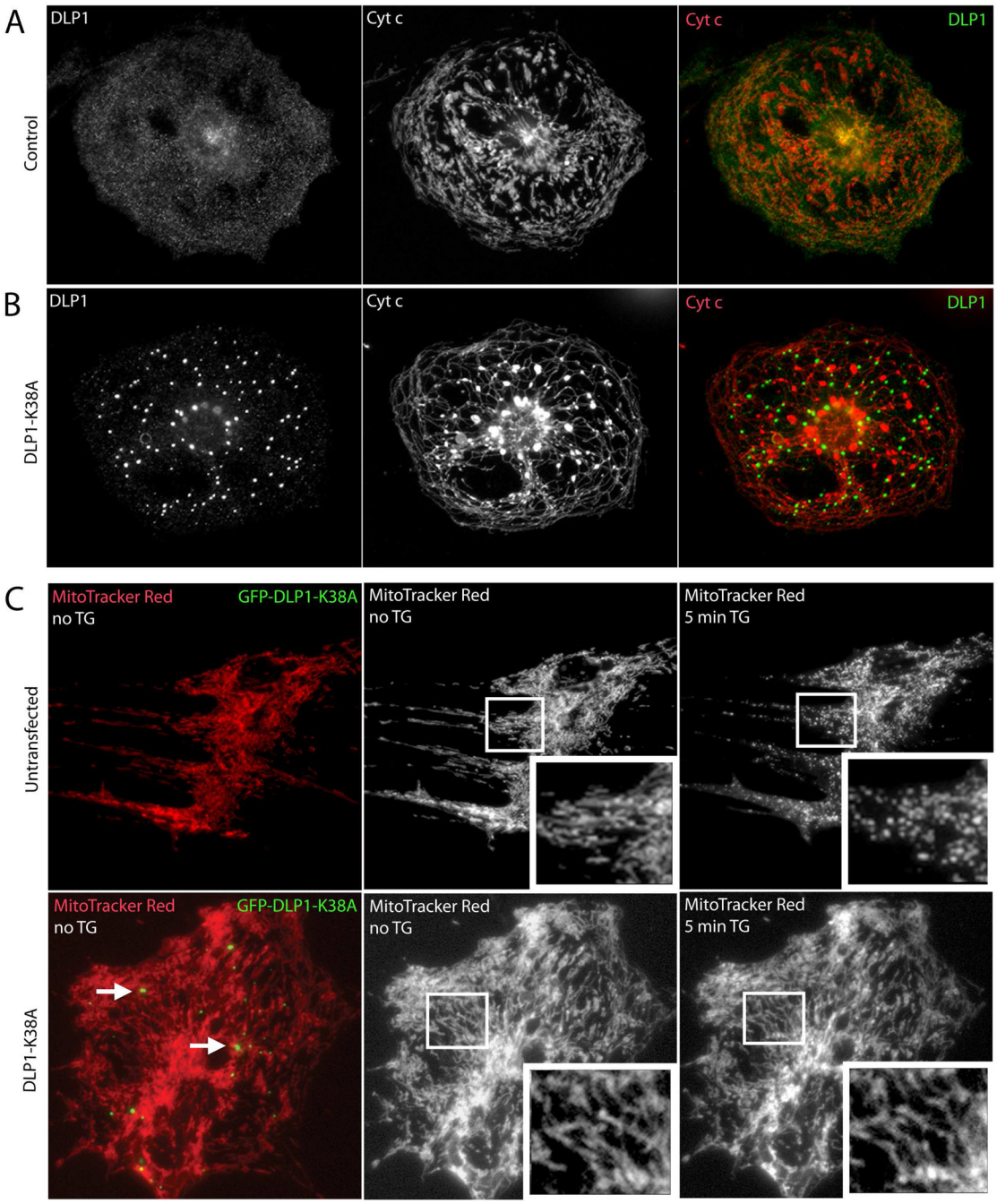

Figure 3. TG-induced mitochondrial fragmentation requires the mitochondrial fission protein DLP1 in neonatal ventricular myocytes

(A) A control neonatal ventricular myocyte labeled with anti-DLP1 and anti-cytochrome *c* antibodies displays diffuse cytosolic DLP1 and a mix of globular and tubular mitochondria, while the overlay shows little association of DLP1 (green) with mitochondria (red). (B) A neonatal ventricular myocyte overexpressing the dominant negative fission mutant, DLP1-K38A, displays large cytosolic aggregates of DLP1, characteristic of mutant DLP1-K38A expression, and elongated and entangled mitochondria [27,29]. The overlay shows that mutant DLP1 aggregates (green) do not colocalize with mitochondria (red). (C) Cells were transfected with GFP-tagged DLP1-K38A and live mitochondria were visualized using MitoTracker Red

CMXRos. The cells that were positive for DLP1-K38A expression were identified by the presence of green mutant DLP1 aggregates (arrows, lower left), while untransfected cells did not display green aggregates (upper left). The mitochondrial network in control, untransfected cells became fragmented upon 5 min TG treatment (top), while TG has no effect on the elongated and tubular mitochondria seen with GFP-tagged DLP1-K38A overexpression (bottom).

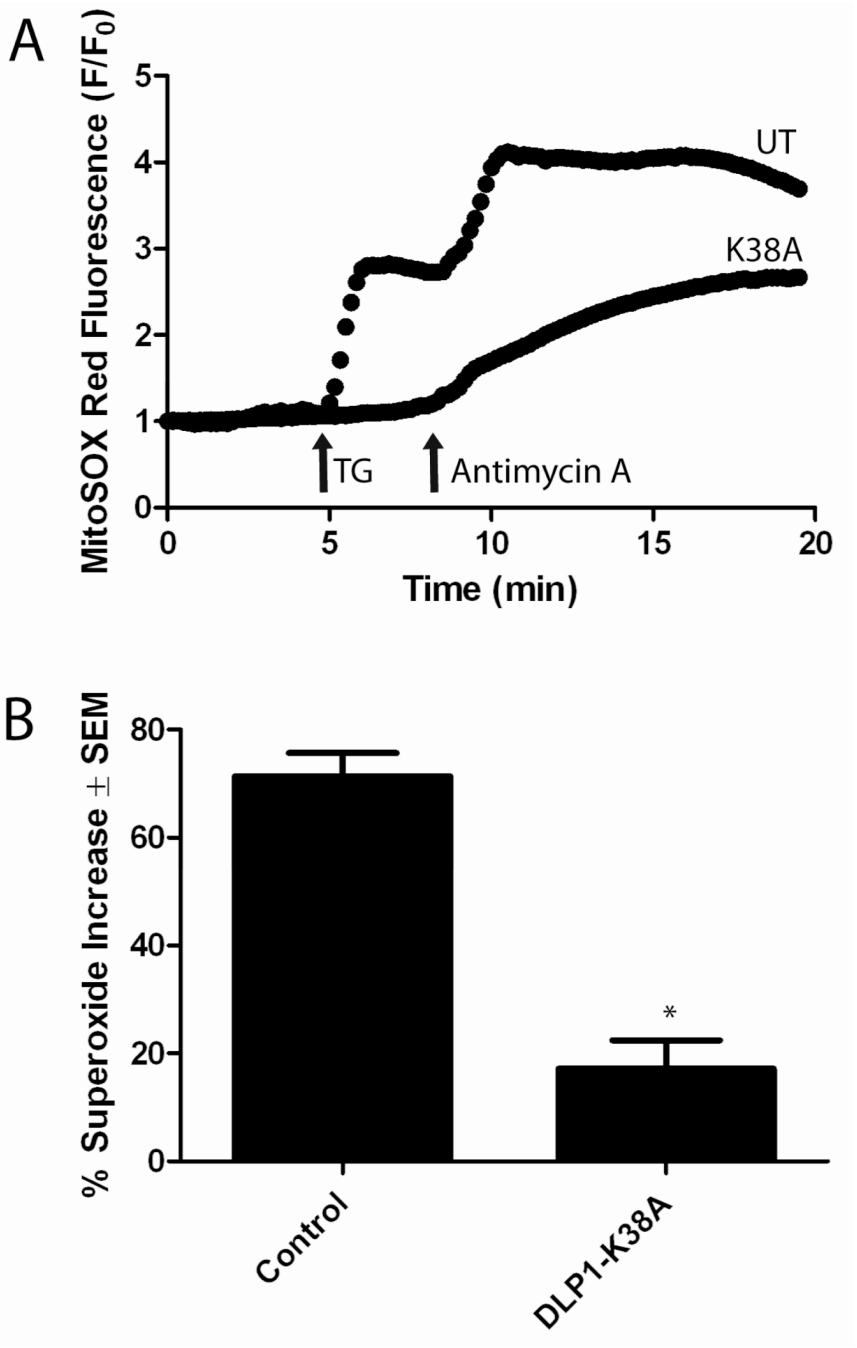

Figure 4. Inhibition of mitochondrial fission prevents Ca^{2+}-induced superoxide increase in neonatal ventricular myocytes

(A) Single traces of superoxide production, measured using MitoSOX Red, show that DLP1-K38A overexpression prevented TG-induced superoxide production but not that caused by 10 μM antimycin A, a mitochondrial complex III inhibitor. (B) Statistical analysis revealed that the increase in superoxide production after TG treatment was significantly decreased in cells expressing DLP1-K38A (* P<0.01, t-test, n=8).